Mathematical Theory and Modeling
ISSN 2224-5804 (Paper) ISSN 2225-0522 (Online)
Vol.7, No.4, 2017

ANALYSIS OF HEAT AND MASS TRANSFER RATES OF HYDROMAGNETIC TURBULENT FLUID FLOW OVER AN IMMERSED INFINITE HORIZONTAL CYLINDER WITH HALL CURRENT

W. O. MUKUNA[1*]; J. K. KWANZA[2]; J. K. SIGEY[2]; J. A. OKELLO[2]

[1]Department of Mathematics and Computer Science, University of Kabianga, P.O Box 2030 KERICHO, 20200, Kenya.

[2]Department of Pure and Applied Mathematics, Jomo Kenyatta University of Agriculture and Technology, P. O. Box 62000 NAIROBI, 00200, Kenya

[*]E-mail of the corresponding author: **okinyimukuna@yahoo.com**

Abstract

A mathematical model of hydromagnetic turbulent boundary layer fluid flow past a horizontal infinite cylinder with Hall current is considered. The cylinder is placed in cross flow with the fluid. The fluid flow is impulsively started and the flow problem is subsequently analysed. The flow is modeled using the momentum, energy and concentration conservation equations. The Reynolds stresses arising due to turbulence in the conservation equations are resolved using Prandtl mixing length hypothesis. The equations are then solved by a finite difference method. The effects of flow parameters on the primary velocity, secondary velocity, temperature and concentration profiles are investigated. It is found that velocity profiles increase with increase in Hall parameter and temperature and concentration profiles increase with increase in magnetic parameter.

Key words: Turbulent flow, Hall current, cylinder, hydromagnetic, convection, finite difference

1. INTRODUCTION

Research in magnetohydrodynamics continues to attract increased interest. This is attributed to the importance of this subject to solving engineering problems. Turbulent flows are increasingly being investigated as most practical fluid flows are turbulent in nature. Verron J. and Sommeria J.,(1987) carried out a numerical simulation of a two-dimensional turbulence experiment in magnetohydrodynamics. The setup consisted of a layer of mercury enclosed in a square box and driven by the injection of electric currents in a uniform magnetic field. The numerical finite difference model was used to simulate the Navier–Stokes equation in two

dimensions with steady forcing and linear bottom friction.

Kim S. J. and Lee C. M. (2002), carried out an investigation of the flow around a circular cylinder under the influence of an electromagnetic force. In their investigation, the effect of the local electromagnetic body force on the flow behavior around a circular cylinder was conducted. Benim et al (2008) modelled turbulent flow past a circular cylinder by RANS, URANS, LES and DES. Dousset V. and Potherat A.,(2008) presented their work on numerical simulation of a cylinder wake under a strong axial magnetic field. They studied the flow of a liquid metal in a square duct past a circular cylinder in a strong externally imposed magnetic field. Kwanza et al, (2010) presented a study on a mathematical model of turbulent convective fluid flow past a vertical infinite plate with hall current. They investigated a magnetohydrodynamics (MHD) turbulent boundary layer fluid flow past a vertical infinite plate in a dissipative fluid with Hall current. They concluded that increase in Hall parameter led to increase in velocity profiles. They used Prandtl mixing length hypothesis to resolve turbulence stress terms in the momentum equation. Dawit et al (2014) did an analysis of turbulent hydromagnetic flow with radiative heat over a moving vertical plate in a rotating system . Rashid A. Ahmad (1996) presented his work on steady-state numerical solution of the Navier-Stokes and energy equations around a horizontal cylinder at moderate reynolds numbers from 100 to 500 . In his work a numerical analysis of forced-convection heat transfer from a horizontal stationary circular cylinder dissipating a uniform heat flux in a cross flow of air was conducted. The full two-dimensional steady-state Navier-Stokes and energy equations in the range of the Reynolds numbers from 100 to 500 (based on diameter) were solved. Yoon H. S. et al, (2004) carried out a numerical study on the fluid flow and heat transfer around a circular cylinder in an aligned magnetic field. They numerically investigated a two-dimensional laminar fluid flow and heat transfer past a circular cylinder in an aligned magnetic field using the spectral method to ensure the accuracy of results. Emmah M et al (2012) presented a study on hydromagnetic turbulent flow past a semi-infinite vertical plate subjected to heat flux. They found out that Hall current significantly affected the velocity of a fluid flow.

In the current investigation a study is carried out on turbulent fluid flow over an infinite horizontal cylinder in the presence of a strong magnetic field.

2. Mathematical model

A two dimensional turbulent boundary layer flow is considered. The fluid flow is transverse to a horizontal infinitely long cylinder lying in the x-y plane. The cylinder is immersed in the fluid. The axis of the cylinder is in the positive x-axis direction and the fluid flows from positive y-axis direction orthogonal to the axis of the cylinder. The vertical axis is the z-axis. The cylinder is assumed to have non-end effects. The fluid is assumed incompressible and viscous. A strong magnetic field of uniform strength H_0 is applied along the x-axis. The induced magnetic field is considered negligible hence $\mathbf{H} = (H_0, 0, 0)$. The temperature of the surface of the cylinder and the fluid are assumed to be the same initially. At time $t^* > 0$ the fluid starts moving impulsively with velocity U_0 and at the same time the temperature of the cylinder is

instantaneously raised to T_W^* which is maintained constant later on. Given that the flow is over a cylinder, cylindrical coordinate form of the governing equations are used. The flow is considered to be along the angular and axial components. There is no radial flow. Thus the two dimensions of this flow are θ and x.

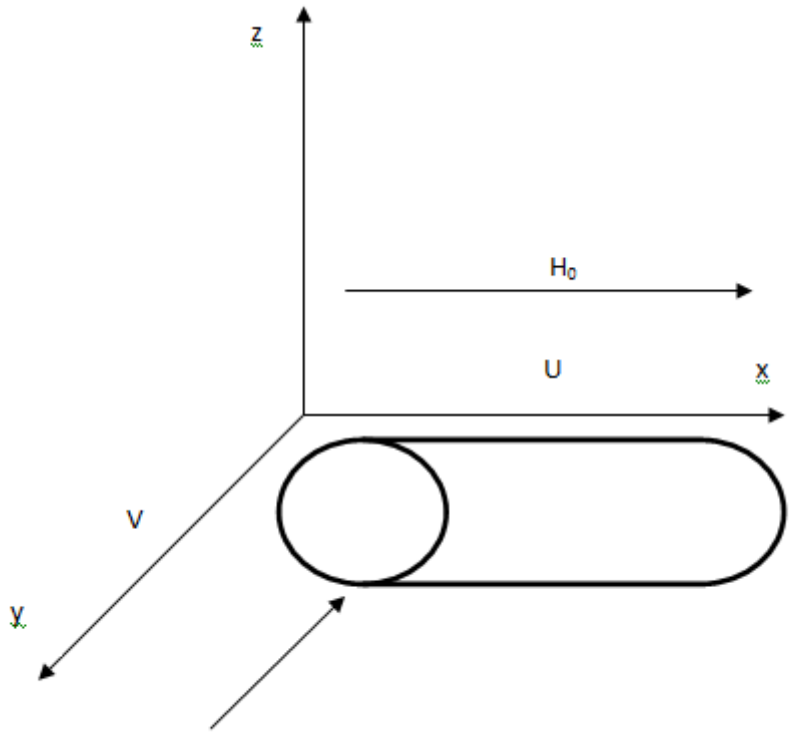

Figure 1: Schematic diagram for the fluid flow

The above flow is governed by the following cylindrical coordinate equations:

$$\frac{\partial \overline{U_\theta^*}}{\partial t^*} = \nu\left(\frac{\partial^2 \overline{U_\theta^*}}{\partial r^{*2}} + \frac{1}{r^*}\frac{\partial \overline{U_\theta^*}}{\partial r^*} - \frac{\overline{U_\theta^*}}{r^{*2}}\right) - \left[\frac{\partial \overline{U_r' U_\theta'}}{\partial r^*} - \frac{2\overline{U_\theta' U_r'}}{r^*}\right] + \vec{J} \times B\big|_\theta \quad (1)$$

$$\frac{\partial \overline{U_x^*}}{\partial t^*} = +\nu\left[\frac{\partial^2 \overline{U_x^*}}{\partial r^{*2}} + \frac{1}{r^*}\frac{\partial \overline{U_x^*}}{\partial r^*}\right] - \left[\frac{1}{r^*}\frac{\partial \overline{U_x' U'}_r}{\partial r*}\right] + J \times B\big|_x \quad (2)$$

$$\rho C_p\left(\frac{\partial \overline{T^*}}{\partial t^*}\right) = k\left(\frac{\partial^2 \overline{T^*}}{\partial r^{*2}} + \frac{1}{r*}\frac{\partial \overline{T^*}}{\partial r^*}\right) - \rho C_p\left(\frac{\partial (\overline{U_r' T'})}{\partial r^*}\right) \quad (3)$$

$$\left(\frac{\partial \overline{C^*}}{\partial t^*}\right) = D\left(\frac{\partial^2 \overline{C^*}}{\partial r^{*2}} + \frac{1}{r^*}\frac{\partial \overline{C^*}}{\partial r^*}\right) - \left(\frac{\partial (\overline{U_r' C'})}{\partial r}\right) \quad (4)$$

The boundary and initial conditions are:

$t^* < 0 : U_\theta{}^* = 0, U_x{}^* = 0, T^* = T_\infty^*, C = C_\infty^*$ everywhere (5a)

$t^* \geq 0 : U_\theta{}^* = U_0, U_x{}^* = 0, T^* = T_W^*, C = C_W^*$ at $r = \frac{D}{2}$ (D is the diameter) (5b)

$U_\theta{}^* \to 0, U_x{}^* \to 0, T^* \to T_\infty^*, C \to C_\infty^*$ as $r \to \infty$ (5c)

The equation of conservation of charge $\nabla . J = 0,$ gives $j_r = k$, a constant, where $\vec{J} = (j_r, j_\theta, j_z)$. The constant is zero since, $j_r = 0$ at the cylinder which is electrically non-conducting. Thus $j_r = 0$ everywhere in the flow. Neglecting the ion-slip and thermoelectric effects, generalized Ohm's law including the effects of Hall current (Cowling T. G. (1957)) gives:

$$\vec{J} + \frac{w_e \tau_e}{H_0}(\vec{J} \times \vec{H}) = \sigma\left(\vec{E} + \mu_0 \vec{q} \times \vec{H} + \frac{1}{en_e}\nabla P_e\right) \quad (6)$$

For the problem we seek to solve there is no applied electric field hence $\vec{E} = 0$ and thus neglecting electron pressure, equation (6) becomes:

$$\vec{J} + \frac{w_e \tau_e}{H_0}(\vec{J} \times \vec{H}) = \sigma\mu_0\left(\vec{q} \times \vec{H}\right) \quad (7)$$

Given that $\vec{H} = (H_0, 0, 0)$ and taking $\vec{J} = (0, j_\theta, j_z)$, $\vec{q} = (0, U_\theta, U_z)$ and $\vec{B} = \mu_0 \vec{H}$ simplifying equation (7) and solving gives:

$j_r = 0$ (8a)

$$j_\theta = \frac{\sigma\mu_0 H_0 (U_z + mU_\theta)}{1 + m^2} \quad (8b)$$

$$j_z = \frac{\sigma\mu_0 H_0 (mU_z - U_\theta)}{1 + m^2} \quad (8c)$$

Where $m = w_e \tau_e$ is the Hall parameter.

Thus the electromagnetic force along θ and x-axis from (8) are respectively:

$$(J \times B)_\theta = \frac{\sigma \mu_0^2 H_0^2 (mU_z - U_\theta)}{1+m^2} \tag{9a}$$

$$(J \times B)_x = \frac{-\sigma \mu_0^2 H_0^2 (U_z + mU_\theta)}{1+m^2} \tag{9b}$$

Hence the governing equations (1) and (2) are respectively:

$$\frac{\partial \overline{U_\theta^*}}{\partial t^*} = \nu \left(\frac{\partial^2 \overline{U_\theta^*}}{\partial r^{*2}} + \frac{1}{r^*} \frac{\partial \overline{U_\theta^*}}{\partial r^*} - \frac{\overline{U_\theta^*}}{r^{*2}} \right) - \left[\frac{\partial \overline{U_r' U_\theta'}}{\partial r^*} - \frac{2\overline{U_\theta' U_r'}}{r^*} \right] + \frac{\sigma \mu_0^2 H_0^2 (m\overline{U_x^*} - \overline{U_\theta^*})}{1+m^2} \tag{10}$$

$$\frac{\partial \overline{U_x^*}}{\partial t^*} = \nu \left[\frac{\partial^2 \overline{U_x^*}}{\partial r^{*2}} + \frac{1}{r^*} \frac{\partial \overline{U_x^*}}{\partial r^*} \right] - \left[\frac{1}{r^*} \frac{\partial \overline{U_x' U'_r}}{\partial r^*} \right] - \frac{\sigma \mu_0^2 H_0^2 (\overline{U_x^*} + m\overline{U_\theta^*})}{1+m^2} \tag{11}$$

2.1 NON-DIMENSIONALIZATION

We non-dimensionalize equations (3), (4), (10) and (11). The following scaling variables are applied in the non-dimensionalization process:

$$t = \frac{U_0 t^*}{D}; r = \frac{r^*}{D}; U_i = \frac{U_i^*}{U_0}; \theta = \frac{T^* - T_\infty^*}{T_w^* - T_\infty^*} \quad C = \frac{C^* - C_\infty^*}{C_w^* - C_\infty^*} \tag{12 a,b,c,d,e}$$

Substituting this scaling variables and introducing non-dimensional parameters gives:

$$\frac{\partial U_\theta}{\partial t} = \frac{1}{\mathrm{Re}} \left(\frac{\partial^2 U_\theta}{\partial r^2} + \frac{1}{r} \frac{\partial U_\theta}{\partial r} - \frac{U_\theta}{r^2} \right) - \frac{\partial \overline{U_r' U_\theta'}}{\partial r} + \frac{\overline{2U_\theta' U_r'}}{r} + M^2 \,\mathrm{Re} \frac{(mU_x - U_\theta)}{1+m^2} \tag{13}$$

$$\frac{\partial U_x}{\partial t} = \frac{1}{\mathrm{Re}} \left(\frac{\partial^2 U_x}{\partial r^2} + \frac{\partial U_x}{r \partial r} \right) - \left[\frac{1}{r} \frac{\partial \overline{U_x' U_r'}}{\partial r} \right] - M^2 \,\mathrm{Re} \frac{(U_x + mU_\theta)}{(1+m^2)} \tag{14}$$

$$\frac{\partial \theta}{\partial t} = \frac{1}{\mathrm{Pr}.R} \left(\frac{\partial^2 \theta}{\partial r^2} + \frac{1}{r} \frac{\partial \theta}{\partial r} \right) - \frac{\partial (\overline{U_r'' \theta'})}{\partial r} \tag{15}$$

$$\left(\frac{\partial C}{\partial t} \right) = \frac{1}{Sc.\mathrm{Re}} \left(\frac{\partial^2 C}{\partial r^2} + \frac{1}{r} \frac{\partial C}{\partial r} \right) - \left(\frac{\partial (\overline{U_r' C'})}{\partial r} \right) \tag{16}$$

Where:

$$\mathrm{Re} = \frac{U_0 D}{\nu}$$

$$Sc = \frac{\nu}{D}$$

$\mathrm{Pr} = \mu C_p / k$

$$M^2 = \frac{\sigma \mu_0^2 H_0^2 \nu}{U_0^2}$$

Boundary and Initial Conditions

From equation 12 the non-dimensional form of 5 becomes:

$$t < 0 : U_\theta = 0, U_x = 0, \theta = 0, C = 0 \text{ everywhere} \quad (17a)$$

$$t \geq 0 : U_\theta = 1, U_x = 0, \theta = 1, C = 1 \text{ at } r = \frac{1}{2} \quad (17b)$$

$$U_\theta \to 0, U_x \to 0, \theta \to 0, C \to 0 \text{ as } r \to \infty \quad (17c)$$

2.2 Resolving Reynolds stress terms

The Reynolds stresses in the energy and mass conservation equations are computed in terms of Turbulent Prandtl number and Turbulent Schmidt number respectively. We write the momentum stress terms as functions of, r, θ, x, U_θ and U_x i.e we need a function F such that :

$$\overline{U_r' U_\theta'} = F(\theta, r, x, U_\theta, U_x)$$

Adopting the Boussinessque approximation:

$$\tau_t = -\rho \overline{U'_\theta U'_r} = A_\tau \frac{\partial U_\theta}{\partial r}$$

Considering Prandtl mixing length hypothesis we have

$$\rho \overline{U'_\theta U'_r} = -\rho l^2 \left(\frac{\partial U_\theta}{\partial r} \right) \left(\frac{\partial U_\theta}{\partial r} \right)$$

At this stage further assumptions are taken:

a) for $r^+>5$ we neglect the viscous term in the shear stress,

b) $l = kr$ where k is the von Karman constant, sometimes referred to as the Karman constant (McComb(1994)).

We thus have:

$$\overline{U'_\theta U'_r} = -k^2 r^2 \left(\frac{\partial U_\theta}{\partial r}\right)\left(\frac{\partial U_\theta}{\partial r}\right) \tag{18}$$

and

$$\overline{U'_x U'_r} = -k^2 r^2 \left(\frac{\partial U_x}{\partial r}\right)\left(\frac{\partial U_x}{\partial r}\right) \tag{19}$$

The turbulent Prandtl number is defined as:

$$\mathrm{Pr}_t = \frac{\xi_M}{\xi_H}$$

From the mixing length hypothesis it can be deduced that:

$$\xi_M = -k^2 r^2 \frac{\partial U_\theta}{\partial r}$$

Thus the model equations become:

$$\frac{\partial U_\theta}{\partial t} = \frac{1}{\mathrm{Re}}\left(\frac{\partial^2 U_\theta}{\partial r^2} + \frac{1}{r}\frac{\partial U_\theta}{\partial r} - \frac{U_\theta}{r^2}\right) + 2k^2 r^2 \left(\frac{\partial U_\theta}{\partial r}\right)\left(\frac{\partial^2 U_\theta}{\partial r^2}\right) + M^2 \,\mathrm{Re}\,\frac{(mU_x - U_\theta)}{1+m^2} \tag{20}$$

$$\frac{\partial U_x}{\partial t} = \frac{1}{\mathrm{Re}}\left(\frac{\partial^2 U_x}{\partial r^2} + \frac{\partial U_x}{r\partial r}\right) + 2k^2\left(\frac{\partial U_x}{\partial r}\right)^2 + 2k^2 r\left(\frac{\partial U_x}{\partial r}\right)\left(\frac{\partial^2 U_x}{\partial r^2}\right) - M^2\,\mathrm{Re}\,\frac{(U_x + mU_\theta)}{(1+m^2)} \tag{21}$$

$$\frac{\partial \theta}{\partial t} = \frac{1}{\mathrm{Pr}.R}\left(\frac{\partial^2 \theta}{\partial r^2} + \frac{1}{r}\frac{\partial \theta}{\partial r}\right) - \frac{k^2 r^2}{\mathrm{Pr}_t}\left(\frac{\partial U_\theta}{\partial r}\right)\left(\frac{\partial^2 \theta}{\partial r^2}\right) \tag{22}$$

$$\left(\frac{\partial C}{\partial t}\right) = \frac{1}{Sc.\mathrm{Re}}\left(\frac{\partial^2 C}{\partial r^2} + \frac{1}{r}\frac{\partial C}{\partial r}\right) - \frac{k^2 r^2}{Sc_t}\left(\frac{\partial U_\theta}{\partial r}\right)\left(\frac{\partial^2 C}{\partial r^2}\right) \tag{23}$$

3. Finite Difference Scheme

In the following finite difference scheme the primary velocity U_θ is denoted by U and the secondary velocity U_r is denoted by V to reduce the subscripts as we use i and j as subscripts, i corresponds to r as j corresponds to t. The equivalent finite difference schemes for equations (20) – (23) are respectively:

$$U_{(i,j+1)} = U_{(i,j)} + \frac{\Delta t}{\mathrm{Re}}\left(\frac{U_{(i+1,j)} - 2U_{(i,j)} + U_{(i-1,j)}}{(\Delta r)^2} + \frac{1}{i\Delta r}\frac{U_{(i+1,j)} - U_{(i,j)}}{\Delta r} - \frac{U_{(i,j)}}{(i\Delta r)^2}\right) +$$

$$2k^2(\Delta t)(i\Delta r)^2\left(\frac{U_{(i+1,j)} - U_{(i,j)}}{\Delta r}\right)\left(\frac{U_{(i+1,j)} - 2U_{(i,j)} + U_{(i-1,j)}}{(\Delta r)^2}\right) + M^2(\Delta t)\mathrm{Re}\frac{\left(mV_{(i,j)} - U_{(i,j)}\right)}{1+m^2} \qquad (24)$$

$$V_{(i,j+1)} = V_{(i,j)} + \frac{\Delta t}{\mathrm{Re}}\left(\frac{V_{(i+1,j)} - 2V_{(i,j)} + V_{(i-1,j)}}{(\Delta r)^2} + \frac{1}{i\Delta r}\frac{V_{(i+1,j)} - V_{(i,j)}}{\Delta r}\right) + \quad 2\Delta t k^2\left(\frac{V_{(i+1,j)} - V_{(i,j)}}{\Delta r}\right)^2 +$$

$$2k^2 i(\Delta t)(\Delta r)\left(\frac{V_{(i+1,j)} - V_{(i,j)}}{\Delta r}\right) \quad \left(\frac{V_{(i+1,j)} - 2V_{(i,j)} + V_{(i-1,j)}}{(\Delta r)^2}\right) - \quad M^2\,\mathrm{Re}(\Delta t)\frac{\left(V_{(i,j)} + mU_{(i,j)}\right)}{1+m^2}$$

(25)

$$\theta_{(i,j+i)} = \theta_{(i,j)} + \frac{\Delta t}{\mathrm{Pr}.\mathrm{Re}}\left(\frac{\theta_{(i+1,j)} - 2\theta_{(i,j)} + \theta_{(i-1,j)}}{(\Delta r)^2} + \frac{1}{i\Delta r}\frac{\theta_{(i+1,j)} - \theta_{(i,j)}}{\Delta r}\right) +$$

$$\frac{k^2(\Delta t)(i\Delta r)^2}{\mathrm{Pr}_t}\left(\frac{U_{(i+1,j)} - U_{(i,j)}}{\Delta r}\right)\left(\frac{\theta_{(i+1,j)} - 2\theta_{(i,j)} + \theta_{(i-1,j)}}{(\Delta r)^2}\right) \qquad (26)$$

$$C_{(i,j+1)} = C_{(i,j)} + \frac{\Delta t}{Sc.\mathrm{Re}}\left(\frac{C_{(i+1,j)} - 2C_{(i,j)} + C_{(i-1,j)}}{(\Delta r)^2} + \frac{1}{i\Delta r}\frac{C_{(i+1,j)} - C_{(i,j)}}{\Delta r}\right) +$$

$$\frac{k^2(\Delta t)(i\Delta r)^2}{Sc_t}\left(\frac{U_{(i+1,j)} - U_{(i,j)}}{\Delta r}\right)\left(\frac{C_{(i+1,j)} - 2C_{(i,j)} + C_{(i-1,j)}}{(\Delta r)^2}\right) \qquad (27)$$

The boundary and initial conditions (17) now take the form:

$$j < 0 : U_{(i,j)} = 0, V_{(i,j)} = 0, \theta_{(i,j)} = 0, C_{(i,j)} = 0 \text{ everywhere} \qquad (28a)$$

$$j \geq 0 : U_{(i,j)} = 1, V(i,j) = 0, \theta_{(i,j)} = 1, C_{(i,j)} = 1 \text{ at } i = \frac{1}{2}\nabla r \qquad (28b)$$

$$U_{(i,j)} \to 0, V_{(i,j)} \to 0, \theta_{(i,j)} \to 0, C_{(i,j)} \to 0 \text{ as } i \to \infty \qquad (28c)$$

These were solved and the results displayed in graphs. The results were analyzed and the analyses are given below.

4.0 Determination of skin friction, the rate of heat transfer and the rate of mass transfer

Skin friction, the rate of heat transfer and the rate of mass transfer are determined from the velocity, temperature and concentration profiles and given in tables. The rate of heat and mass transfer are given by

$Nu = -\left.\frac{\partial \theta}{\partial r}\right|_{r=0.5}$ and $Sh = -\left.\frac{\partial C}{\partial r}\right|_{r=0.5}$ respectively.

The skin friction is given by, Rathy (1976),

$\tau_u = -\left.\frac{\partial U}{\partial r}\right|_{r=0.5}$ and $\tau_v = -\left.\frac{\partial \mathrm{V}}{\partial r}\right|_{\mathrm{r}=0}$ where $\tau = \frac{\tau^*}{\rho U^2}$

The above are calculated by numerical differentiation using Newton's interpolation formula over the first five points.

$$\tau_x = \frac{5}{6}\left[25u(0,i) - 48u(1,i) + 36u(2,i) - 16u(3,i) + 3u(4,i)\right] \quad (29)$$

$$\tau_y = \frac{5}{6}\left[25v(0,i) - 48v(1,i) + 36v(2,i) - 16v(3,i) + 3v(4,i)\right] \quad (30)$$

$$Nu = \frac{5}{6}\left[25\theta(0,i) - 48\theta(1,i) + 36\theta(2,i) - 16\theta(3,i) + 3\theta(4,i)\right] \quad (31)$$

$$Sh = \frac{5}{6}\left[25C(0,i) - 48C(1,i) + 36C(2,i) - 16C(3,i) + 3C(4,i)\right] \quad (32)$$

5.0 DISCUSSION OF RESULTS

The primary velocity, secondary velocity, temperature and concentration profiles are presented graphically in figures 2 – 5 while skin friction, rate of heat transfer and rate of mass transfer are presented in tables 1 – 3.

5.1 Primary velocity

From figure 2 we observe that:

(i) Increase in Magnetic parameter leads to decrease in primary velocity profiles. Increase in Magnetic parameter implies magnetic force subdues the inertial force of the fluid thus the decrease in primary velocity profile.

(i) The primary velocity profiles decreases with increase in Reynolds number. This is due to the fact that as Reynolds Number increases the viscous effects are lessened consequently the boundary layer diminishes and the fluid assumes the free stream velocity.

(iii) The primary velocity profiles increases with increase in Hall parameter this is due to the fact that the effective conductivity decreases with the increase in Hall parameter which reduces the magnetic damping force hence the increase in velocity. It is also clear from the model equations that the Hall parameter directly affects the primary velocity.

(iv) The primary velocity profiles increase with increase in time parameter. This is because as time increases the flow approaches the free stream region hence assuming the free stream velocity.

(v) Prandtl number and Schmidt number do not affect the velocity profiles.

5.2 Secondary Velocity

From figure 3 we observe that:

(i) Secondary velocity profiles decreases with increase in Magnetic number. This is caused by the fact that increase in Magnetic number implies magnetic force is more significant over inertial force hence increase in Magnetic number subdues velocity.

(ii)Increase in Reynolds number decreases secondary velocity profiles. As Reynold’s number increases the viscous effects diminish hence the boundary layer also diminishes.

(iii) Secondary velocity profiles increase with increase in Hall parameter.

(iv) The secondary velocity profiles increase with increase in time parameter just as for the case with primary velocity as time increases the flow approaches the free stream region hence assuming the free stream velocity.

(v) Prandtl number and Schmidt number do not affect the velocity profiles.

5.3 Temperature

In figure 4 the first three curves of colours red, blue and black coincide and appear as black. From this figure it is noted that:

(i) Increase in Prandtl number leads to decrease in temperature profiles. Increase in Prandtl number implies decrease in thermal diffusion hence reduction in temperature profiles.

(ii) There is no change in temperature profiles with variation in Reynolds number and Magnetic parameter. This is clear as from the model equation the Reynolds number does not directly affect temperature equation.

(iii) The profiles increase with increase in time parameter. This implies as time increases the temperature increase thus the temperature is time dependent as it is in the model.

(iv) Variation in Hall parameter and Schmidt number do not affect Temperature profiles as the two parameters do not have an aspect that relates to temperature.

5.4 Concentration

From figure 5 it is observed that

(i) Increase in Magnetic and Reynolds numbers does not affect concentration profiles. This shows that the contribution of this two parameters to concentration through velocity is

negligible.

(iii) Concentration profiles decrease with increase in Schmidt number. Increase in Schmidt number implies decrease in mass diffusion thus the reduction in concentration profiles.

(iv) The profiles increase with increase in time parameter. This is because the concentration profiles are time dependent thus as time increases they increase.

(v) Variation in Hall parameter and Prandtl number were found not to affect concentration profiles thus they were kept constant.

5.5 Skin friction

From table 1 it is observed that:

i) An increase in magnetic parameter leads to a decrease in the skin friction τ_u. This is occasioned by the increase in primary velocity profile which implies decrease in skin friction when magnetic parameter is increased.

ii) The skin friction τ_v increases with increase in magnetic parameter. τ_u

iii) An increase in Hall parameter leads to a decrease in both skin frictions τ_u and τ_v. This is due to the fact that increase in Hall parameter increases the velocity and therefore shear resistance is decreased.

iv) An increase in Reynolds number leads to a decrease in skin friction τ_u as high Reynold's number implies increased inertial force hence increased velocity.

(v) Skin friction τ_v increases with increase in Reynolds number. Secondary velocity profiles are reduced by Reynold's number due to increase of shear stress τ_v.

vi) An increase in time parameter leads to a decrease in skin friction τ_u as time parameter

increases velocity but does not have an observable effect on skin friction τ_v.

5.6 Heat transfer rate

From table 2 it is noted that:

i) A variation in magnetic parameter, Reynolds number or time parameter does not affect the rate of heat transfer.

ii) An increase in Prandtl number leads to an increase in the rate of heat transfer. Increase in Prandtl number implies decrease in thermal diffusion hence increase in rate of heat transfer.

5.7 Mass transfer rate

From table 3 it is noted that:

i) A variation in magnetic parameter, Reynolds number or time parameter does not affect the rate of mass transfer.

ii) An increase in Schmidt number leads to an increase in the rate of mass transfer. Increase in Schmidt number implies decrease in mass diffussion hence increase in rate of mass transfer.

6.0 Conclusion

The finite difference method used in this paper has made it possible to transform the highly nonlinear partial differential equations into discrete form to obtain their approximate solutions.

From the preceding discussion of results, it can be concluded that a strong magnetic field subdues turbulence as it generally decreases velocity profiles. Hall current also affects the

primary velocity as it causes an increase in primary velocity profiles. It is observed that change in Hall parameter has no effect on temperature neither concentration. Clearly primary velocity, secondary velocity, temperature and concentration increase with time. The resolution of turbulence terms as done by use of the Prandtl mixing length hypothesis and use of turbulent Schmidt number and turbulent Prandtl number has been validified by this results as they are consistent with previous researches carried out for example by Kwanza (2010) and Marigi (2012).

References

Ahmad R. A. (1996); Steady-State Numerical Solution of the Navier-Stokes and Energy Equations around a Horizontal Cylinder at Moderate Reynolds Numbers from 100 to 500. *Heat Transfer Engineering Volume 17, Issue 1,*

Benim A.C., Pasqualotto E., Suh S.H.;(2008) Modelling turbulent flow past a circular cylinder by RANS, URANS, LES and DES.; *International Journal of Computational Fluid Dynamics, Volume 8, Number 5/2008 pp 299-307*

Cowling T.G., (1957) Magnetohydrodynamics *New York: Interscience,*.

Dousseta V. and Poth ératb A.(2008),Numerical simulations of a cylinder wake under a strong axial magnetic field; *Physics of fluids 20, 017104*

Gebre D. H., Makinde O. D. and Kinyanjui M.(2014); Analysis of Turbulent Hydromagnetic Flow with Radiative Heat over a Moving Vertical Plate in a Rotating System. *Applied and Computational Mathematic . Vol. 3, No. 3, , pp. 100-109.*

Kim S. J. and Lee C. M., (2002), Numerical Investigation of cross flow around a circular cylinder at a low Reynolds number flow under an electromagnetic force. *KSME International journal Vol. 16 No. 3 pp 363 – 375*

Kwanza J.K.; Mukuna W. O. and Kinyanjui M.(2010); A mathematical model of turbulent convective fluid flow past a vertical infinite plate with Hall current.; *International Journal of Modelling and Simulation, Vol. 30, No. 3* , pg 376- 386

Marigi E., Kinyanjui M. and Kwanza J.(2012); Hydromagnetic turbulent flow past a semi-infinite vertical plate subjected to heat flux. *Mathematical Theory and Modeling Vol.2, No.8, pp 15 – 25.*

McComb W.D. (1994), The physics of fluid turbulence *New York: Oxford Science Publications,*.

Verron J. and Sommeria J., (1987). Numerical simulation of a two-dimensional turbulence experiment in magnetohydrodynamics. *Physics of Fluids Vol. 30, pp 732- 747*

Yoon H. S., Chun H. H., Ha M. Y., and Lee H. G.(2004); A numerical study on the fluid flow and heat transfer around a circular cylinder in an aligned magnetic field.; *Int. J. Heat Mass Transfer 47, 4075*

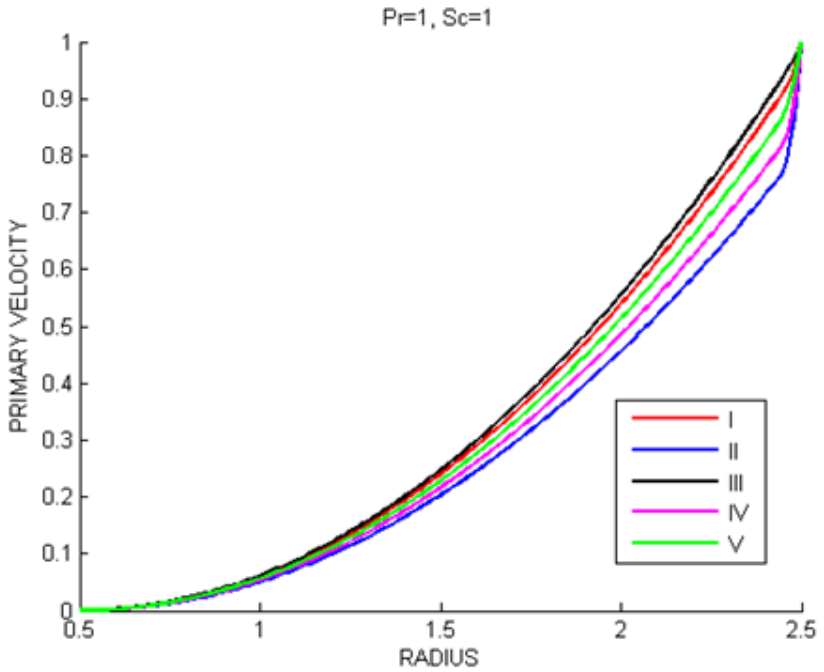

	M^2	m	Re	t
I	2	2	5e3	0.2
II	4	2	5e3	0.2
III	2	4	5e3	0.2
IV	2	2	1.5e4	0.2
V	2	2	5e3	0.4

Figure 2 Primary velocity profiles

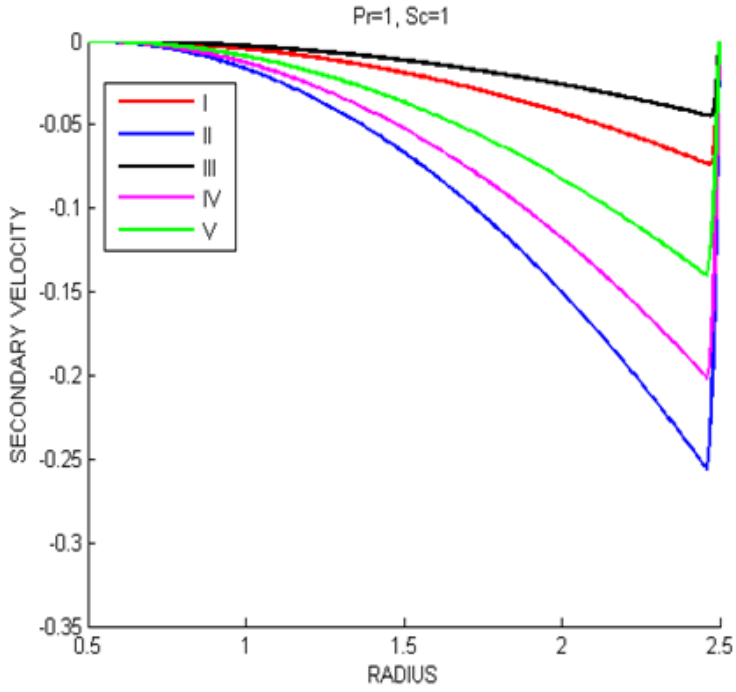

	M^2	m	Re	t
I	2	2	5e3	0.2
II	4	2	5e3	0.2
III	2	4	5e3	0.2
IV	2	2	1.5e4	0.2
V	2	2	5e3	0.4

Figure 3 Secondary velocity profiles

	M^2	Re	Pr	t
I	2	5e3	1	0.2
II	4	5e3	1	0.2
III	2	1.5e4	1	0.2
IV	2	5e3	5	0.2
V	2	5e3	1	0.4

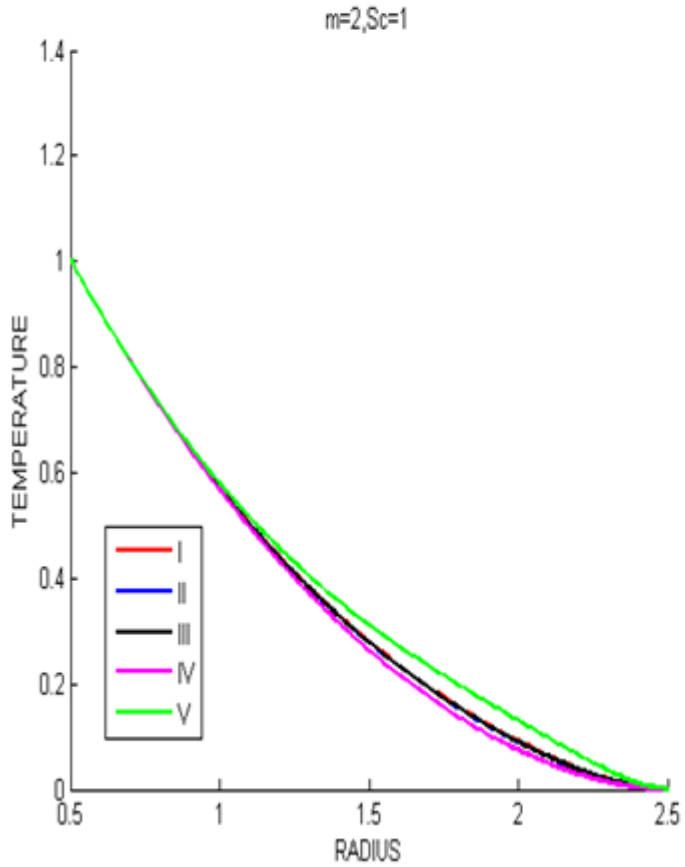

Figure 4 Temperature profiles

	M^2	Re	Sc	t
I	2	5e3	1	0.2
II	4	5e3	1	0.2
III	2	1.5e4	1	0.2
IV	2	5e3	5	0.2
V	2	5e3	1	0.4

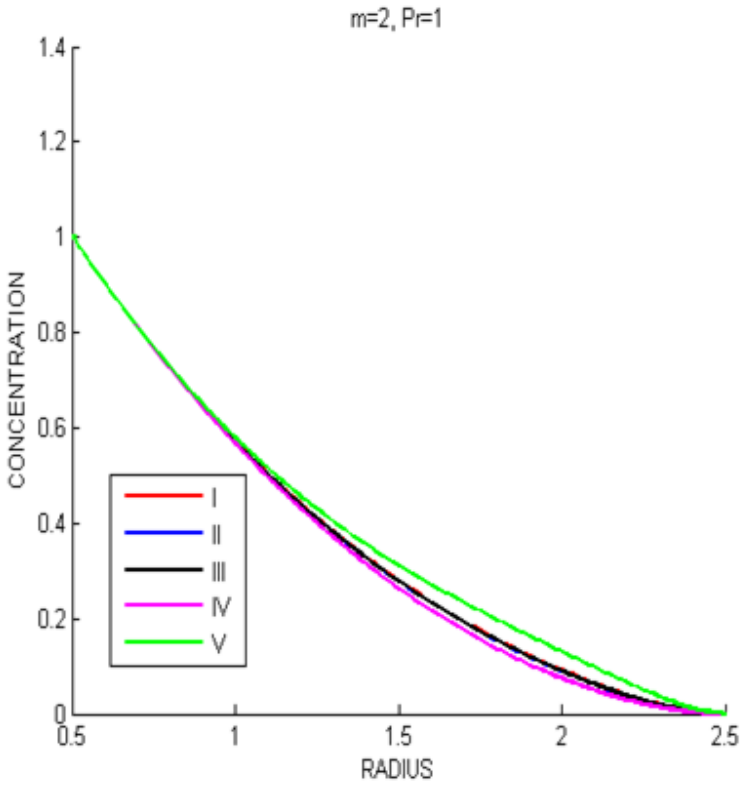

Figure 5 Concentration profiles

Table 1 Skin friction

	M^2	m	Re	t	τ_u	τ_v
I	2	2	5e3	0.2	0.0046	0.0013
II	4	2	5e3	0.2	0.0026	0.0053
III	2	4	5e3	0.2	0.0002	0.0008
IV	2	2	1.5e4	0.2	0.0020	0.0040
V	2	2	5e3	0.4	0.0007	0.0013

Table 2 Heat transfer rates

	M^2	Re	Pr	t	Nu
I	2	5e3	1	0.2	-0.0008
II	4	5e3	1	0.2	-0.0008
III	2	1.5e4	1	0.2	-0.0008
IV	2	5e3	5	0.2	-0.0003
V	2	5e3	1	0.4	-0.0008

Table 3 Mass transfer rates

	M^2	Re	Sc	t	Sh
I	2	5e3	1	0.2	-0.0008
II	4	5e3	1	0.2	-0.0008
III	2	1.5e4	1	0.2	-0.0008
IV	2	5e3	5	0.2	-0.0003
V	2	5e3	1	0.4	-0.0008

	The first author, Wilys O. Mukuna was born 1977 in Western Kenya. He holds a Bachelor of Science Degree with Honours and a Master of Science degree in Applied Mathematics. He is currently a lecturer at the Department of Mathematics and Computer Science, University of Kabianga, Kenya and a Doctoral Student at Jomo Kenyatta University of Agriculture and Technology, Kenya.
	Jackson K. Kwanza, the second author was born in 1963 in Eastern Kenya. He holds a PhD degree in Applied Mathematics. He is a Professor of Applied Mathematics at the Department of Pure and Applied Mathematics, Jomo Kenyatta University of Agriculture and Technology (JKUAT), Kenya and has Supervised many postgraduate students. His research interests are in the areas of fluid dynamics and numerical analysis. He was the Director of Continuing Education Programme between 2003 and 2006 and he is currently the Principal Karen Campus, JKUAT.
	The third author, Johana K. Sigey was born in South Rift Valley Kenya. He holds a PhD degree in Applied Mathematics. He is a Professor of Applied Mathematics at the Department of Pure and Applied Mathematics, Jomo Kenyatta University of Agriculture and Technology, JKUAT, Kenya and has supervised many Doctoral and Master students besides teaching undergraduate courses. His research interests are in fluid mechanics. He was Chairman of Department of Pure and Applied Mathematics between 2003 and 2008, JKUAT and is currently the Director Kisii CBD Campus, JKUAT.
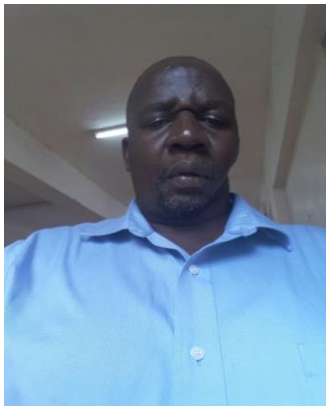	Born in Western Kenya Nyanza, the fourth author, Jeconiah A. Okelo holds a Doctoral degree in Applied Mathematics. He is a Senior Lecturer of Applied Mathematics at the Department of Pure and Applied Mathematics, Jomo Kenyatta University of Agriculture and Technology, JKUAT, Kenya and has supervised several Postgraduate students besides teaching undergraduate courses. His research interests are in fluid mechanics. He is currently the Deputy Director of School of Distance and e-Learning, JKUAT, Kenya.